Analysis of Design Parameters For Shunt Valve and Anti-Siphon Device Used to Treat Patients with Hydrocephalus

Jong Yun Jang, Chang Min Suh
School of Mechanical Engineering, Kyungpook National University, Daegu 702-701, Korea
Chong Sun Lee*
School of Mechanical and Control System Engineering, Handong Global University, Kyungbuk 791-708, Korea

The present study investigated design parameters of shunt valves and anti-siphon device used to treat patients with hydrocephalus. The shunt valve controls drainage of cerebrospinal fluid (CSF) through passive deflection of a thin and small diaphragm. The anti-siphon device (ASD) is optionally connected to the valve to prevent overdrainage when the patients are in the standing position. The major design parameters influencing pressure-flow characteristics of the shunt valve were analyzed using ANSYS structural program. Experiments were performed on the commercially available valves and showed good agreements with the computer simulation. The results of the study indicated that predeflection of the shunt valve diaphragm is an important design parameter to determine the opening pressure of the valve. The predeflection was found to depend on the diaphragm tip height and could be adjusted by the diaphragm thicknesss and its elastic modulus. The major design parameters of the ASD were found to be the clearance (gap height) between the thin diaphragm and the flow orifice. Besides the gap height, the opening pressure of the ASD could be adjusted by the diaphragm thickness, its elastic modulus, area ratio of the diaphragm to the flow orifice. Based on the numerical simulation which considered the increased subcutaneous pressure introduced by the tissue capsule pressure on the implanted shunt valve system, optimum design parameters were proposed for the ASD.

Key Words : Shunt Valve, Anti-Siphon Device (ASD), Hydrocephalus, Cerebrospinal Fluid (CSF), Siphon Effect, Subcutaneous Pressure

1. Introduction

Cerebrospinal fluid (CSF) is secreted from the choroid plexus in the ventricles enclosed by the brain and its volume is around 200cc. The CSF circulates in the ventricle, subarachnoid space, and the spinal cord to protect brain and carry out metabolic wastes. It is produced about 500cc a day (20 cc/hr) and finally absorbed to the cerebral vein enclosing the subarachnoid space (Kent and Van, 1984). In case secretion and absorption of the CSF is not properly controlled for some reason, the ventricles expand and pressurize the brain. This symptom is called hydrocephalus and can cause death if not properly treated.

Various kinds of shunt valves have been developed to treat hydrocephalus since Pudenz introduced a silicone valve in 1950's which shunted the accumulating CSF to the proper site of the body such as the peritoneal cavity (Drake and Saint-Rose, 1995). The currently available shunt valves were mostly designed in 1980's and have successfully contributed to treat patients with hydrocephalus. However, there are several prob-

* Corresponding Author,
E-mail : cslee@han.ac.kr
TEL : +82-54-260-1393 ; **FAX** : +82-54-260-1312
Associate Professor, Department of Mechanical and Control Engineering, Handong Global University, 3 Namsong-ri, Heunghae-eub, Buk-gu, Pohang City, Kyungbuk 791-708, Korea.

lems present with the shunt systems, which are obstruction in the shunt system, infection, valve malfunction, and over-drainage of CSF due to siphon effect(Post, 1985). The patency of the currently available shunt system is known to be around 50% in 5 years. Therefore, researches are in progress to solve the problems involved with current shunt systems and enhance qualities of the shunt products.

There are about one hundred thousands shunt valves are consumed worldwide and two thousands and five hundreds of shunt valves are being imported in Korea every year. Although various types of shunt valves are operated by neuro surgeons in Korea, researches are few concerning functional characteristics of shunt systems and their selection appropriate to the patient conditions. Literatures are not available yet worldwide that shows detailed analysis of design parameters in relation to the functional characteristics of the shunt valves(Lee and Jang, 2000 ; Won et al., 2001).

In this study, we numerically analyzed important design parameters of the shunt valves and anti-siphon devices with regard to their pressure-flow control characteristics. They were appropriately modeled and simulated to understand influence of each design variable on the magnitude of the valve opening pressure. We also simulated CSF under-drainage conditions due to increase in the subcutaneous pressure by the so called tissue capsule phenomenon following implantation of ASD. Our simulations were applied to the commercially available shunt system and the results were compared with the experimental data. Based on the simulation, optimal values of the design parameters were derived for the anti-siphon device considering the tissue capsule pressure.

2. Working Principles of Shunt Valves and Anti-Siphon Devices

2.1 Shunt valves

Depending on the site of implantation, shunt valves are categorized into three types: ventriculoperitoneal(VP) valve, lumboperitoneal (LP) valve, and ventriculoatrial(VA) valve (Drake and Saint-Rose, 1995). Because VP valves are mostly used by surgeons, our study is being focused on these valves. As shown in Fig. 1, VP valve is implanted under the scalp between neck and cupola. A 10-15cm length of inlet catheter(ventricular catheter) is connected between the inlet port of the valve and the ventricle. An anti-siphon device(ASD) is optionally connected to the outlet port of the valve. The outlet catheter is connected to the outlet port of the valve or ASD and the tip of the outlet catheter is located to the peritoneal cavity through inner skin area. Therefore, the CSF accumulated in the ventricle is drained into the peritoneal cavity.

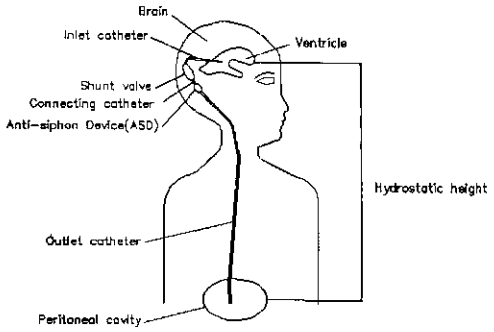

Fig. 1 Ventriculoperitoneal(VP) shunt system (valve plus catheters)

Several types of shunt valves are commercially available in the market. In the present study, we employed a constant-pressure type shunt valve that controls CSF with a small silicone diaphragm. These valves currently dominate the market and is displayed in Fig. 2. The outer body (dome) of the valve is made of flexible silicone elastomer while the inner part(base) is made of rigid plastic. The thin elastic diaphragm is seated in the plastic base and controls the flow. The diaphragm works like a check valve. It opens when the ventricular pressure gets a certain level and is closed at lower ventricular pressures, and prevent back flow of the CSF. Shunt valves are characterized by the design and performance of this tiny flow regulating element(Lee and Jang, 2000).

The lower part of Fig. 2 shows diaphragm design and the resulting pressure-flow curve. The

diaphragm opens when the ventricular pressure is increased above a threshold value (called opening pressure), and hence prevent further increase in the ventricular pressure. This valve is called constant pressure type valve because variations in the pressure are small for the wide range of flow rate. Consequently, the ventricular pressure of the patient with this valve can be controlled almost constant irrespective of the CSF flow rate.

A predeflection (height difference between surface A and B in Fig. 2) is given in the valve design to prevent CSF drainage before the ventricle gets a certain level of pressure, which is the opening pressure. When the ventricular pressure exceeds this level, the diaphragm deflects below the contact surface with the plastic base to form a flow orifice. Then, the CSF begin to flow. Therefore, the opening pressure is a major design parameter for the shunt valve.

2.2 Anti-siphon devices (ASD)

When a patient with a constant pressure type shunt valve stands up or sits and stays in these positions, CSF overdrainage occurs due to siphon effect. Anti-siphon devices are used to prevent such an over-drainage phenomenon. A few different ASD products have been introduced in the market. Currently, the ASD dominating the market employs a thin diaphragm to prevent over-drainage.

Figure 3 shows a schematic of a diaphragm type ASD and Fig. 4 demonstrates its working principles. In case the patient stays in the standing position, negative pressure develops under the central region (orifice region) of the diaphragm due to the siphon effect of the outlet catheter. Atmospheric pressure prevails on the upper-surface of the diaphragm because ASD is implanted under the scalp which is in contact with the atmosphere. This pressure difference deflects the thin diaphragm towards the orifice and blocks it to prevent over-drainage of the CSF. Without the ASD, the negative pressure developing in the outlet catheter pulls up the CSF and causes over-drainage. The over-drainage problem involved with shunt valves is known to be adapted by 80% of patients. However, for the remaining 20% patients, it causes severe problems such as silt ventricles.

If the ASD chamber pressure is raised over a

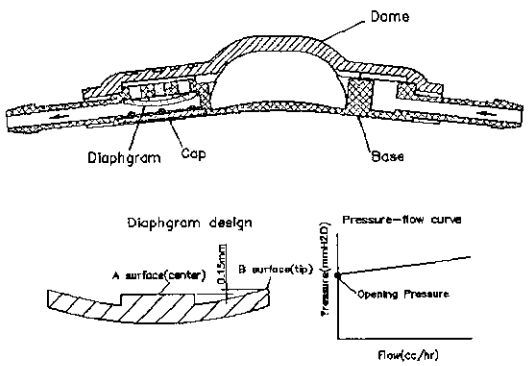

Fig. 2 Schematics of the diaphragm type shunt valve

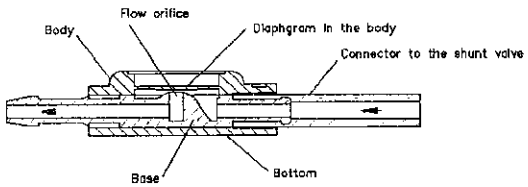

Fig. 3 Schematics of the Anti-siphon device (ASD)

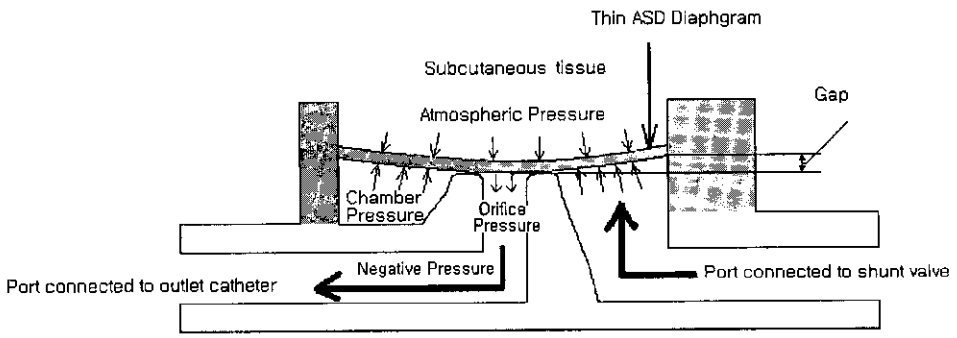

Fig. 4 Working principles of ASD

certain level following the increase of the ventricular pressure, the diaphragm deflects upward and the orifice is reopened to drain the CSF. This threshold pressure is called an opening pressure of ASD. The opening pressure depends on the patient posture because the posture alters the siphon height and hence the magnitude of the negative pressure developing in the outlet catheter. ASD's are categorized into a normally open type and a normally closed type. The normally open type allows a gap between the diaphragm and the orifice in the supine position whereas the normally closed type does not allow the gap. The magnitude of the gap height is an important design parameter for adjusting the opening pressure of the ASD as will be analyzed in the following sections.

3. Method of Numerical Simulation and Experiment

3.1 Numerical simulation of shunt valve

Pressure-flow characteristics of a diaphragm type shunt valve is almost determined by the design of the small diaphragm. Therefore, the diaphragm was selected as a simulation model in the present study. The purpose of the simulation is to calculate the required displacement enough to initiate CSF flow when a given opening pressure acts on the upper surface of the diaphragm. As the tip(indicated by B in Fig. 2) of the diaphragm is displaced below the height of surface A, the diaphragm opens and the CSF begin to flow through the orifice formed between the diaphragm tip and the surface of the base which has been in contact with the diaphragm. Based on the simulation, the required height difference between surface A and B could be determined for a given opening pressure by trial and error technique.

Figure 5 shows both the undeformed and deformed shapes of the axisymmetric finite element model of the valve diaphragm simulated by the ANSYS structural analysis program. We employed axisymmetric 8-node solid ANSYS elements(plane 82) because the diaphragm(6.0 mm in diameter) is axisymmetric in geometry as well as in loading conditions. Symmetric boundary conditions were applied along the central axis of the diaphragm. The pressure boundary condition equal to the opening pressure was specified on the upper surface of the diaphragm. The lower surface of the diaphragm was assumed to be in the atmospheric pressure and hence zero gage pressure condition was specified. Total 436 elements were enough to accurately solve the static elasticity problem.

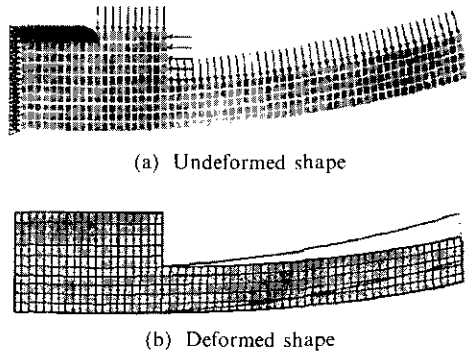

(a) Undeformed shape

(b) Deformed shape

Fig. 5 FEM model of the shunt valve diaphragm

Large deformation option was employed with 10 substeps because strains were computed as much as a few precents and the change in the geometry was substantial. We used Poisson' ratio of 0.49 considering incompressibility of the silicone elastomer. Although the silicone elastomers are a hyper elastic material showing S-shaped stress-strain curves for a wide range of strains up to almost 1000%, we assumed a constant elastic modulus and used an average value in the slope between 0 and 5% strains considering the fact that the shunt valves experience strains within a few percent. Our test showed the average elastic modulus within 5% strains ranged between 1.5 MPa and 10.0 MPa for Q7 series medical grade elastomers depending on their hardness numbers. Radius of curvature of the diaphragm was 9.0 mm and three different diaphragm thicknesses used for the simulation were 0.30, 0.45, 0.70 mm.

3.2 Numerical simulation of ASD

Figure 6 shows both the undeformed and deformed shapes of the axisymmetric finite element model of the ASD diaphragm. The diameter of the diaphragm was 6.0 mm and its thickness

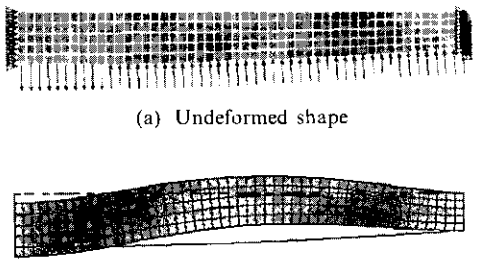

(a) Undeformed shape

(b) Deformed shape

Fig. 6 FEM model of the ASD diaphragm

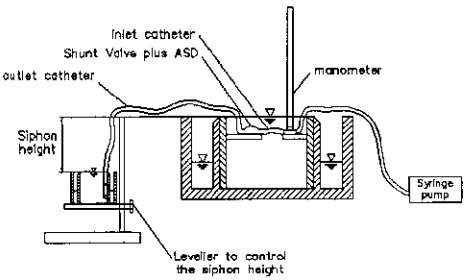

Fig. 7 Experimental set-up for testing ASD

varied between 0.2 mm and 0.3 mm. Symmetric boundary conditions were specified on the central axis of the diaphragm. The outer edge of the diaphragm was specfied with zero displacement considering the edge was attached to the ASD body and its movement was almost restricted. Zero gage pressure was specified on the upper surface of the diaphragm.

When the patient is in the standing position, negative pressure develops on the central portion (1.1 mm diameter flow orifice area) of the lower surface of the diaphragm due to siphon effect. Therefore, we gave negative hydrostatic pressures on this region corresponding to the siphon height. Figure 6 shows the central portion of the diaphragm to be deflected downward by the negative pressure developed by the siphon effect, which is a typical phenomenon for patients in the standing position because of the water colume height difference between the ventricle and the site of CSF drainage(peritoneal cavity). As the chamber pressure is increased to a certain level, the orifice reopens. The purpose of the present simulation is to determine the chamber pressure required to reopen the orifice. The problem was solved by changing the chamber pressure to find the pressure when the central portion of the diaphragm is displaced as much as the gap size.

In the present study, we assumed a shunt valve with a medium pressure level to be connected to the inlet port of the ASD. Therefore, the ventricular pressure necessary to open the shunt valve and ASD was obtained by simply adding the known opening pressure of the medium range shunt valve, 80 mmH_2O, to the computed chamber pressure required to open the ASD diaphragm at the given siphon heights. Similar to the shunt valve simulation, we employed axisymmetric 8-node solid ANSYS element to solve the static elasticity problem. Total 257 elements were used with large deformation option. The same mechanical properties(Poisson's ratio and constant elastic modulus) were used as the shunt valves.

The most important design parameter for the ASD is the gap size, which represents the distance between the lower surface of the diaphragm and the upper surface of the flow orifice. Zero gap size and negative gap size(−0.1 mm) were simulated for the normally closed type ASD whereas 0.1 and 0.2 mm gap sizes were simulated for the normally open type ASD. We applied a 30 mmH_2O of subcutaneous pressure to the upper surface of the diaphragm to investigate the influence of ASD encapsulation by the surrounding tissues on the ASD opening pressure and delineate the clinically reported under-drainage problem(Drake et al., 1993 ; Hassan et al., 1996).

3.3 Experimental method of ASD

We performed in-vitro experiments using a Radionics ASD. A Radionics shunt valve with a medium pressure range were connected to the ASD to obtain valve opening pressure. The purpose of the experiment was to validate our numerical solution. The experiments were performed according to ISO 7197 protocol which specifies standard procedures for testing shunt valves and ASD's. Figure 7 shows an experimental set-up used in the study. As specified in ISO7197, we measured the opening pressure of the shunt valve and ASD assembly using a manometer by manually lowering the height of the outlet catheter from 0 upto 50 cm. These operations induced

siphon effect on the outlet catheter resulting in the negative hydrostatic pressure to develop in the proximal side of the outlet catheter. Therefore, the pressure in the outlet flow orifice of the ASD was decreased from 0 cmH_2O upto -50 cmH_2O.

4. Results and Discussions

4.1 Numerical simulation of shunt valve

In order to determine the required amount of predeflection of the diaphragm tip, we calculated displacement of the tip for three different ranges in the opening pressure: 30 mmH_2O for a low pressure, 80 mmH_2O for a medium pressure, 145 mmH_2O for a high pressure. Table 1 shows the results of our simulation for a range of diaphragm thickness and elastic modulus. The amount of deflection decreased as the diaphragm thickness and elastic modulus were increased, which means higher opening pressures are required to initiate flow through thicker and stiffer diaphragm. For a shunt valve with 3.0MPa of elastic modulus and 0.45 mm diaphragm thickness (6 mm in diameter), predeflection was computed to be 0.089 mm for the medium pressure range, 80 mmH_2O.

4.2 Numerical simulation of ASD

Figure 8 shows the results of numerical simulation for the ASD diaphragm with uniform thickness ($t=0.3$ mm). We varied the gap size between the diaphragm and the flow orifice, and varied the diaphragm thickness, its elastic modulus and the area ratio (refer to Fig. 4; the ratio of the lower surface area of the diaphragm in which the chamber pressure prevails and the orifice area in which negative pressure develops in the standing position of the patients). The vertical axis in Fig. 8 represents the ventricular pressure required to open the ASD and shunt valve assembly. In order to obtain the opening pressure, the computed ASD chamber pressure required to open the diaphragm was simply added to the opening pressure of the shunt valve with a medium pressure range, 80 mmH_2O.

In Fig. 8(a), the opening pressure is observed to increase as the magnitude of negative hydrostatic pressure in the outlet catheter is raised following the siphon height increase. This is because the higher the siphon height is, the more the negative pressure develops in the proximal side of the outlet catheter and the more strongly the thin diaphragm is pulled downward. Therefore, higher pressure needs to develop in the ASD chamber to overcome the elastic force and open the diaphragm. The raised flow resistance increased the opening pressure by as much as 75 mmH_2O at -50cm of siphon height for the normally closed type ASD.

The gap size was designed to be positive for the normally open type ASD. Due to the presence of this positive gap, which renders the ASD chamber to communicate with the proximal side of the outlet catheter, the opening pressure decreased as the siphon height was increased until the diaphragm blocks the flow orifice. The above region was illustrated by the negative slope in the opening pressure curve in Fig. 8. After passing this siphon height, which we named a critical siphon height (critical point), the opening pressure increased showing a positive slope as the siphon height was further raised. This was because of the loss of communication between the ASD chamber and the distal catheter. Therefore, the opening pressure reached its minimum at the critical

Table 1 Computed predeflection of the shunt valve diaphragm

opening pressure / diaphragm thickness	30 mmH_2O		80 mmH_2O		145 mmH_2O	
	E=1.5 MPa	E=3.0 MPa	E=1.5 MPa	E=3.0 MPa	E=1.5 MPa	E=3.0 MPa
0.30 mm	0.186 mm	0.083 mm	0.566 mm	0.265 mm	0.834 mm	0.520 mm
0.45 mm	0.066 mm	0.032 mm	0.188 mm	0.089 mm	0.361 mm	0.169 mm
0.70 mm	0.024 mm	0.012 mm	0.065 mm	0.032 mm	0.120 mm	0.059 mm

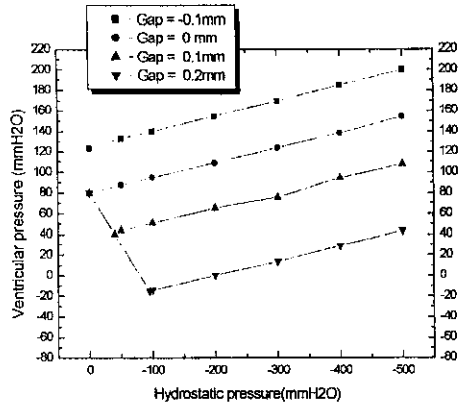

(a) Effect of gap size
(E=1.5 MPa, t=0.30 mm)

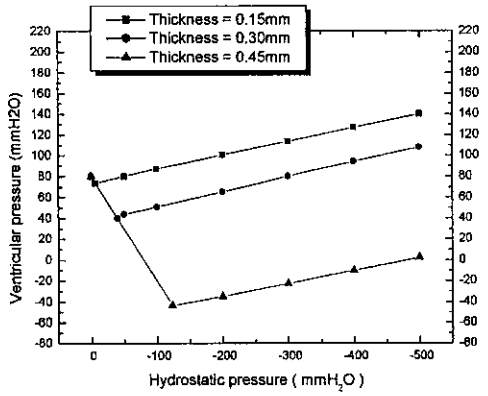

(b) Effect of diaphragm thickness(t)
(E=1.5 MPa, gap=0.1 mm)

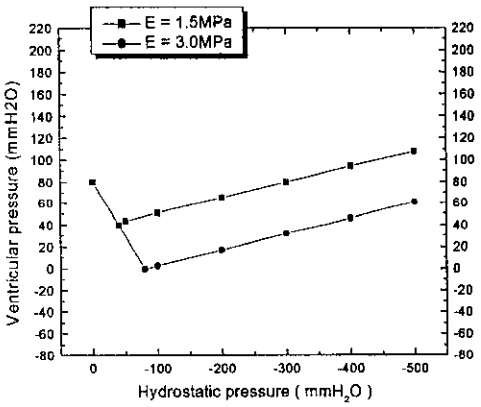

(c) Effect of elastic modulus
(gap=0.1 mm, t=0.30 mm)

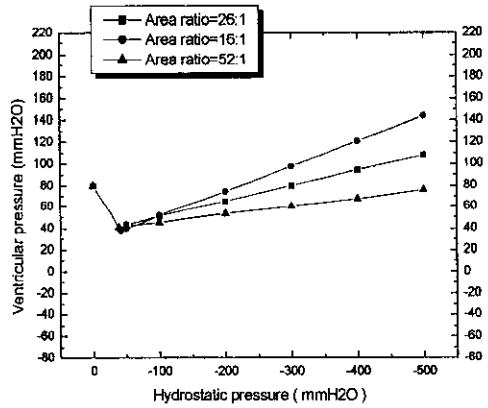

(d) Effect of area ratio
(E=1.5 MPa, gap=0.1 mm, t=0.30 mm)

Fig. 8 Influence of the ASD design parameters on the opening pressure

siphon height. Because of the pressure drop near the critical point, the normally open type ASD showed an opening pressure in the standing position (-50 cmH_2O) only a slightly larger compared to the case of zero siphon. Remember there was no critical pressure observed for the normally closed type ASD due to zero or negative gap height. As the gap size was further raised from 0.1 mm to 0.2 mm, the opening pressure at -50cmH_2O decreased by about 70 mmH_2O. The increased gap height lowered the critical pressure as low as -10 mmH_2O. And the opening pressure at -50 cmH_2O siphon height was by 40 mmH_2O lower than the opening pressure at zero siphon. For the normally open type ASD, one can not escape the presence of the critical pressure. However, we can get a desirable critical pressure (lowest opening pressure), which is not too low and too high by adjusting the gap height appropriately. Therefore the gap size becomes a major design parameter for the ASD.

Figure 8(b) shows variations in the opening pressure depending on the diaphragm thickness. The deflection of the diaphragm decreased as the thickness was increased. Therefore the critical pressure required to deform the same amount decreased towards negative values. However, there was no change in the positive slope of the opening pressure curve after passing the critical pressure. One can observe that the change in the critical pressure was relatively large as the thickness increased from 0.30 to 0.45 mm compared to

the change observed between 0.15 and 0.30 mm.

Figure 8(c) shows the change in the opening pressure depending on the elastic modulus(E). The deflection of the diaphragm decreased as the elastic modulus was increased. Figure 8(d) shows the change in the opening pressure depending on the area ratio. The area ratio has little effect on the magnitude of the critical pressure. However, it decreased the slope of the pressure curve after passing the critical point. For the area ratio of 52:1, the opening pressure is observed to be almost the same for the case of zero siphon and -50 cmH_2O siphon height. However, one can not design the area ratio too large since it may increase chances for the protein wastes to obstruct the flow orifice.

In summary, we conclude that the magnitude of the critical pressure(lowest siphon pressure) depends on the gap size, diaphragm thickness and its elastic modulus. And the area ratio has an influence on the slope of the opening pressure curve after passing the critical point. Therefore, one can design an diaphragm type ASD with an appropriate opening pressure curve so that the critical pressure may not be too low and the difference in the opening pressure be small when the patient is in the standing position and in the supine position.

4.3 Influence of tissue capsule pressure

The ASD implanted in the subcutaneous region under the scalp is surrounded by neighboring cells and encapsulated. Therefore a capsule pressure is formed surrounding the ASD, which pressurizes the diaphragm. Consequently, the upper surface of the diaphragm is exposed to a higher pressure than the atmospheric pressure. This results in the increased flow resistance of the ASD because the capsule pressure forces the diaphragm to deflect downward and block the flow orifice. This phenomenon causes under-drainage of CSF and was clinically reported by several researchers (Hassan et al., 1996 ; Drake et al., 1993). In order to understand the influence of the tissue capsule pressure, we applied 100 mmH_2O of subcutaneous pressure on the upper surface of the diaphragm and computed the new opening pressure. The result is displayed in Fig. 9. Compared with Fig. 8(a), the opening pressure increased and the critical pressure, which is characteristic of the normally open type ASD, disappeared.

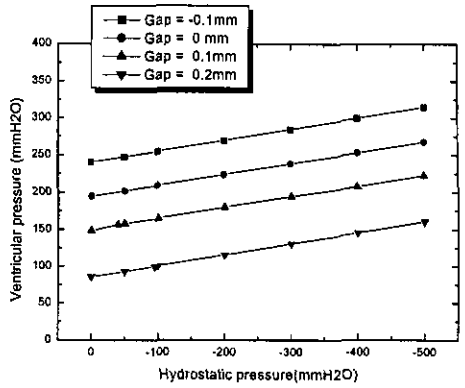

Fig. 9 Opening pressure of the ASD under 100mm H_2O subcutaneous pressure (E=1.5 Mpa, t=0.30 mm)

Therefore one can understand that the increased subcutaneous pressure due to the tissue capsule phenomenon increased the flow resistance in the ASD, and finally caused under-drainage of the CSF. The increase in the subcutaneous pressure nullify the presence of positive gap size, and consequently, the critical pressure did not appear in the opening pressure curve.

4.4 Comparison between simulation and experiment

We employed Radionics shunt valves and ASD's to compare the results of the numerical simulation with the experimental data. These shunt systems were similar to the shunt models analyzed in the present study. The dimensions of the valve and ASD used in the simulation were measured from the commercial Radionics products (6.0 mm ASD diaphragm diameter with 0.3 mm center thickness and 0.17 mm peripheral thickness; 0.08 mm gap height; 3.0 Mpa elastic modulus; 28:1 area ratio). Figure 10 compares the results, which show good agreements between the numerical simulations and experiments as well as the catalog data from Radionics Inc. Similar to the numerical simulation, the experiments showed presence of the critical pressure. However, the critical pressure region is observed to be a little

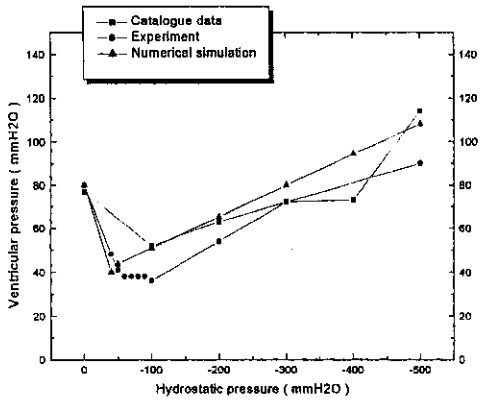

Fig. 10 Comparison of numerical simulations with experiment results and catalogue data for a Radionics ASD connected to a shunt valve with a medium pressure range

wider compared to the sharp point observed in the numerical solution. Similar to the numerical simulation, the opening pressure initially decreased with a negative slope as the siphon height was increased. When the critical pressure was reached, the curve showed a flat pressure zone and then the ventricular pressure increased with the increasing siphon height.

The presence of flat pressure zone near the critical pressure rather than the sharp fall and the quantitative differences in the opening pressure between the experiments and the numerical simulations are attributed to the measurement error in the ASD gap size, non-linearity in the elastic modulus as well as the inherent deviations in the opening pressure which is characteristic of the silicone elastomer products. The Radionics catalogue data showed a similar trend. However, the catalogue data did not accurately reveal the presence of the critical pressure developing close to the supine position, which reduced the opening pressure even in the small siphon height.

4.5 Optimal design parameters of ASD

In summary, we can design an ASD with a desirable opening pressure curve by adjusting gap size, diaphragm thickness, its elastic modulus and area ratio. If the effect of subcutaneous pressure are considered in the early design stage of the ASD, the under-drainage problem may be

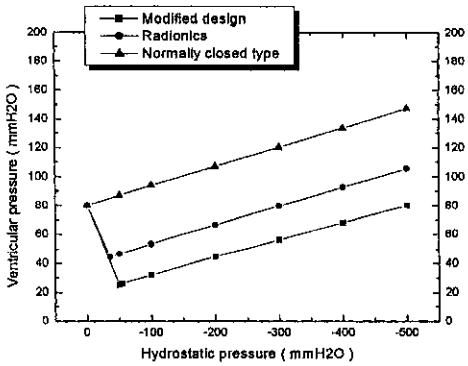

(a) Zero subcutaneous pressure

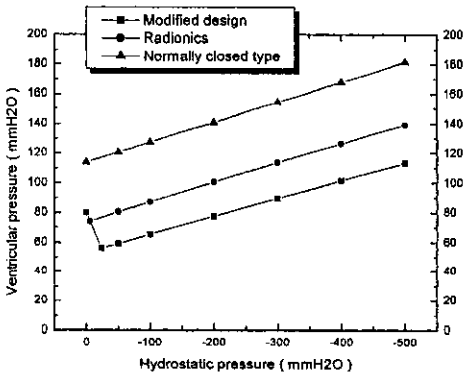

(b) 30mmH_2O subcutaneous pressure

Fig. 11 Comparison between commercial ASD and our modified design

reduced.

Based on the numerical simulation, we slightly modified the values of the design variables for the normally open type ASD. Our design had a 0.12 mm gap size and area ratio of 30:1. The diaphragm diameter was 6.4 mm with its center thickness of 0.30 mm and peripheral thickness of 0.20 mm. Elastic modulus was assumed to be 3.0 Mpa. The results of our modified design were compared with those of Radionic ASD as well as the normally closed type ASD. Figure 11(a) shows the results for the zero subcutaneous pressure whereas Fig. 11(b) shows for the 30 mmH_2O subcutaneous pressure considering the average tissue capsule pressure(Drake and Saint-Rose, 1995).

Our design is a normally open type so that the flow resistance was much smaller than the normally closed type. Compared to the Radionics

ASD, our design had a smaller critical pressure due to the increased gap size and a slightly smaller positive slope in the pressure curve due to 10% larger area ratio. As a result, the difference in the opening pressure between in the supine position and in the standing position was smaller than the Radionics ASD, which renders our design to be more physiological.

5. Conclusion

The structural analysis was performed to understand influences of the major design parameters on the opening pressure characteristics of shunt valves and ASD's used to treat patients with hydrocephalus. The following results were obtained.

(1) The opening pressure, which is a major design parameter influencing pressure-flow characteristics of shunt valves, is determined by the predeflection of the small diaphragm. The opening pressure could be adjusted by appropriately giving the predeflection and selecting the diaphragm thickness and its elastic modulus.

(2) The opening pressure of the ASD was determined by the gap size, diaphragm thickness, its elastic modulus and area ratio. Among these variables, the gap size, diaphragm thickness and the elastic modulus determined magnitude of the critical pressure. On the other hand, the area ratio determined the positive slope of the opening pressure curve after the critical pressure was reached.

(3) The increase in the subcutaneous pressure due to tissue encapsulation after implantation of the ASD caused under-drainage of the CSF. In the normally open type ASD, the increase in the subcutaneous pressure nullify presence of the gap, and hence the critical pressure disappeared in the opening pressure curve.

(4) Based on the results of the present simulation, we determined desirable design parameters for the normally open type ASD. Compared with the normally closed type and the commercially available normally open type ASD, our design is thought to be more physiological because the difference in the opening pressures between in the supine position and in the standing position was almost the same.

(5) The present numerical simulation was validated from the experimental results of the commercial products and their catalogue data.

Therefore we can design shunt valves and ASD's with desirable opening pressure characteristics by applying the present method of simulation properly in the early design stage to reduce the production cost as well as to better design the shunt system.

Acknowledgement

This study was performed by the supports of Ministry of health and welfare through "Development of Implantable Shunt Systems" (HMP-99-E-12-0005) and Brain Korea 21 Mechanical Engineering Unit, Kyungpook National University.

References

Drake, J. M. and Saint-Rose, C., 1995, *The Shunt Book*, New York Blackwell Scientific.

Drake, J. M., Silva, M. C., and Rutka, J. T., 1993, "Functional Obstruction of an Antisiphon Device by Raised Tissue Capsule Pressure," *Neurosurgery*, Vol. 32, pp. 137~139.

Hassan, M., Hagashi, S., Yamashita, J., 1996, "Raised Tissue Capsule Pressure Risks in Using Siphon Reducing Devices in Adult Patients with Normal Pressure," *J. Neurosurgery*, Vol. 84, pp. 634~640.

International Standards, ISO 7197, 1997, "Neurological implants: sterile, single use hydrocephalus shunts and components," 2nd. ed.

Jaeger, K. M. and Layton, T. M., 1997, "New Shunt Concepts for Treatment of Hydrocephalus: in Vitro Testing," The Consensus Conference on Complex Hydrocephalus and Hydrocephalus Complications, Assisi, Italy

Kent, M. and Van, D. G., 1984, "Human Anatomy," Wm. C. Brown Publishers, Dubuque, Iowa.

Lee, C. S., Jang, J. Y., 2000, "Investigation of Shunt Valves Used to Treat Patients with Hydrocephalus," *Journal of Handong Global*

University, Vol. 3, pp. 79~93.

Post, E. M, 1985, "Currently Available Shunt Systems: A Review," *Neurosurgery*, Vol. 16, pp. 257~260.

Watson, D. A., 1992, "The Delta Valve: A Physiologic Shunt System," The Consensus Conference on Pediatric Neurosurgery, Assisi, Italy.

Won, C. S., Hur, N. and Lee, C. S., 2001 "A Flow/Structure Interaction Analysis for the Design of Medical CSF-Flow Control Valve," *Korean Society of Computational Fluid Mechanical Engineering*, Vol. 6, pp. 40~46.